A&A 425, 569–575 (2004)
DOI: 10.1051/0004-6361:20035881

Astronomy & Astrophysics

The frequency evolution of interstellar pulse broadening from radio pulsars

O. Löhmer[1], D. Mitra[1], Y. Gupta[2], M. Kramer[3], and A. Ahuja[4]

[1] Max-Planck-Institut für Radioastronomie, Auf dem Hügel 69, 53121 Bonn, Germany
e-mail: loehmer@mpifr-bonn.mpg.de
[2] National Centre for Radio Astrophysics, TIFR, Pune University Campus, Ganeshkhind, Pune 411007, India
[3] University of Manchester, Jodrell Bank Observatory, Macclesfield, Cheshire SK11 9DL, UK
[4] Inter-University Centre for Astronomy and Astrophysics, Pune University Campus, Ganeshkhind, Pune 411007, India

Received 16 December 2003 / Accepted 23 June 2004

Abstract. In this paper we report multi-frequency measurements of pulse broadening times (τ_d) for nine medium dispersion measure (DM $\approx$ 150–400 pc cm^{-3}) pulsars observed over a wide frequency range. The low frequency data at 243, 325 and 610 MHz are new observations done with the Giant Metrewave Radio Telescope (GMRT). The frequency dependence of τ_d for all but one (PSR B1933+16) of our sources is consistent with the Kolmogorov spectrum of electron density fluctuations in a turbulent medium. PSR B1933+16, however, shows a very flat spectrum as previously observed for high DM pulsars. Our observations combined with earlier published results enable us to study the spectral index of τ_d over the whole observed DM range. While the spectral properties are generally consistent with a Kolmogorov spectrum, pulsars seen along line-of-sights towards the inner Galaxy or complex regions often show deviations from this expected behaviour.

Key words. ISM: structure – scattering – stars: pulsars: general – stars: pulsars: individual: PSR B1933+16

1. Introduction

The free electron density distribution in the interstellar medium (ISM) can be decomposed into three different regimes: the spiral arms consisting of gaint HII regions, the inner disk comprising of a dense ionized region and the thick disk filled with diffuse electron gas (Taylor & Cordes 1993). The pulsar signal traversing the ISM suffers interstellar dispersion quantified in terms of dispersion measure, DM, which is the integrated electron column density towards the pulsar (at distance D), i.e. DM $= \int_0^D \mathrm{n_e}\ \mathrm{dl}$. Fluctuations of the electron density along the line of sight (LOS) give rise to several observable scattering effects, which manifest themselves as observational properties like angular broadening, temporal pulse broadening and scintillation of pulsars (see Rickett 1990, for a review).

Scattering causes propagation of signals along a variety of different ray paths with different geometrical lengths, so that a pulse, which has left the pulsar at one instant, arrives at the observer over a finite time interval. For a Gaussian distribution of irregularities and applying the thin screen approximation, the pulse broadening function (PBF) of the ISM can be well described by an exponential decay of the pulse, i.e. PBF(t) $\sim \exp(-t/\tau_d)$, where τ_d is called the pulse broadening time (Scheuer 1968). Random interference among the different paths produces a diffraction pattern in the plane of the observer. This pattern decorrelates over a characteristic bandwidth $\Delta\nu_d$. Both τ_d and $\Delta\nu_d$ strongly depend on frequency ν (i.e. $\tau_d \propto \nu^{-\alpha}$ and $\Delta\nu_d \propto \nu^{\alpha}$) and are related to each other as

$$2\pi\,\tau_d\,\Delta\nu_d = C_1. \quad (1)$$

The constant C_1 is of the order unity but changes for different models and geometries for the electron density fluctuations (e.g. Lambert & Rickett 1999). However, until now there exists no direct measurement of τ_d and $\Delta\nu_d$ at the same observing frequency for obtaining C_1.

The strength of scattering of radio waves caused by electron density fluctuations in the ISM has been subject of detailed studies since the discovery of scintillation in pulsar signals (Scheuer 1968). A commonly used description of the scattering strength is to attribute a power law to the electron density spectrum with a large range between "inner" and "outer" scales, k_i^{-1} and k_0^{-1}; i.e.,

$$P_{n_e}(q) = \frac{C_{n_e}^2}{(q^2 + k_0^2)^{\beta/2}} \exp\left(-\frac{q^2}{4\,k_i^2}\right), \quad (2)$$

where q is the magnitude of the three-dimensional wavenumber and $C_{n_e}^2$ is the fluctuation strength for a given LOS (e.g. Rickett 1977). For $k_0 \ll q \ll k_i$, one obtains a simple power-law model with a spectral index β, i.e., $P_{n_e}(q) = C_{n_e}^2 q^{-\beta}$ and $\alpha = 2\beta/(\beta - 2)$. For a pure Kolmogorov spectrum of density irregularities, $\beta = 11/3$, we expect $\alpha = 4.4$. Attempts to reconstruct the electron density spectrum from various observations

(Armstrong et al. 1995) have led to the suggestion that over 5 decades of wavenumber range 10^{-13} m^{-1} $< q <$ 10^{-8} m^{-1} the spectrum can be approximated by a power law with an average index $\langle \beta \rangle \sim 3.7$, close to the value expected from the Kolmogorov process. However, there is some evidence for deviations from this picture, over some parts of the wavenumber range (see, for example, Gupta 2000, and references therein).

Furthermore, it is uncertain how the scattering material and processes operate in different directions of the Galaxy. Multi-frequency scatter broadening measurements have been used to determine α for several LOSs in the Galaxy. For LOSs with low DM's (<50 pc cm^{-3}) there is typically good agreement with the Kolmogorov spectrum (Cordes et al. 1985; Johnston et al. 1998). This is also supported by estimates of α in the local ISM using diffractive and refractive interstellar scintillation (ISS) observations of pulsars (Bhat et al. 1999). These local LOSs are most probably sampling the diffuse, homogeneous electron density component of the Galaxy, where the Kolmogorov process holds true. High DM (>400 pc cm^{-3}) pulsars towards the inner parts of the Galaxy, in contrast, have an average $\langle \alpha \rangle = 3.44 \pm 0.13$, showing significant departures from the Kolmogorov spectrum (Löhmer et al. 2001, hereafter Paper I). We interpreted this phenomenon in Paper I as anomalous scattering as discussed by Cordes & Lazio (2001). In this picture the observed anomalous behaviour can be explained by invoking scattering caused by multiple scattering screens with anisotropic irregularities and finite transverse extent along the LOS. As a consequence, less radiation reaches the observer at lower frequencies since some of the radiation that would be scattered by an infinite screen is now lost, causing α to be lower than the standard Kolmogorov value. Indeed, towards these directions at low Galactic latitudes one encounters numerous HII regions embedded in the dense thin disk, so that the probability to find such multiple screens along the LOS is quite high.

In order to get a better understanding of the scattering properties in the ISM we need measurements of α for more LOSs. In particular the scattering properties of intermediate DM pulsars ($100 \lesssim$ DM $\lesssim 400$ pc cm^{-3}) have not been studied yet. In an effort to find α for intermediate DM pulsars we have currently launched an observational program using the Gaint Metrewave Radio Telescope (GMRT) in Pune, India. In this paper we report results for the first phase of these observations.

2. Observations and data analysis

The following selection criteria were used to find an adequate sample of intermediate DM pulsars for our GMRT observations. Firstly pulsars with flux density >10 mJy at 400 MHz were chosen from the Taylor et al. (1993; updated version 1995) catalogue. We also ensured that the expected width of the pulse, i.e. the intrinsic width along with the pulse broadened width, at the lowest frequency (243 MHz) is smaller than 80% of the pulse period. Using an intrinsic pulse width of 5% of the period at ~5 GHz we estimated the width at lower frequencies according to a power-law index of $\lambda^{0.25}$ (e.g. Thorsett 1991), where λ is the wavelength in meters. We found the expected pulse broadening at each frequency by applying the empirical relation τ_d (ms) $= 4.2 \times 10^{-5}$ DM$^{1.6} \times$ $(1 + 3.1 \times 10^{-5}$ DM$^3)$ $\lambda^{4.4}$ (Ramachandran et al. 1997). The final estimated width was found by adding the two widths in quadrature. Applying the above selection criteria we ended up with a sample of 33 pulsars. Here we report results of the first phase of GMRT observations of nine pulsars.

The observations were carried out with the GMRT in February 2002 using three bands around center frequencies at 243, 325 and 610 MHz. The GMRT has a "Y" shaped hybrid configuration of antennas with 14 antennas placed randomly in a compact central array of 1 km by 1 km, and the remaining 16 antennas distributed along the three arms of the "Y" (Swarup et al. 1997). The GMRT was in its commissioning phase during our observations, and due to various maintenance activities not all of the 30 antennas were available for observations. The observations were carried out with typically 20 to 25 antennas. Dual circular polarization signals from all the selected antennas were incoherently added (i.e., signals from each antenna were first detected and then added) in a 256 channel filter bank with a total bandwidth of 16 MHz. The summed signals were integrated to a time constant of 0.516 ms and were recorded for off-line analysis after adding the two polarizations (see Gupta et al. 2000 for more details about the pulsar mode of operation of the GMRT). The filterbank characteristics result in dispersion smearing per channel[1], t_{DM}, for the pulsars observed of 5.7 ms $\leq t_{DM} \leq$ 14.5 ms at 243 MHz, of 2.4 ms $\leq t_{DM} \leq$ 6.1 ms at 325 MHz, and of 0.4 ms $\leq t_{DM} \leq$ 0.9 ms at 610 MHz.

Typical observation times were between 10 and 45 min, depending on the observing frequency and flux density of the individual source. During off-line reduction the filterbank signals were de-dispersed and summed. We analysed the signals for RFI and skipped those parts of the data with spikes larger than a factor of three of the rms of the data. The signals were folded with the topocentric pulse period to produce total power profiles.

At 408 and 1408 MHz we used pulse profiles[2] observed with the 76 m Lovell telescope at Jodrell Bank, UK. Using both circular polarizations the signals were incoherently de-dispersed and added in filterbanks with varying bandwidths. At 408 MHz 32 channels of 0.125 MHz bandwidth (2.4 ms $\leq t_{DM} \leq$ 6.0 ms) were used, and at 1408 MHz 32 channels of 1 MHz each (0.5 ms $\leq t_{DM} \leq$ 1.2 ms) were employed. Details of the system can be found in Gould & Lyne (1998).

In order to measure the pulse broadening time τ_d we used the method described in Paper I. Firstly, we construct a pulse template as a sum of Gaussian components fitted to an observed high frequency profile, where the scattering for the given pulsars is negligible. For our sample, the 1408 MHz profiles were adequate. For each lower frequency, we then find τ_d from the

[1] $t_{DM} = 8.3$ DM $\Delta\nu_{BW}/\nu^3$ μs, where DM is the dispersion measure (pc cm^{-3}), ν is the observing frequency (GHz) and $\Delta\nu_{BW}$ the filterbank channel bandwidth (MHz).

[2] These profiles are publicly available from the European Pulsar Network (EPN) archive maintained by the MPIfR, Bonn, http://www.mpifr-bonn.mpg.de/div/pulsar/data/

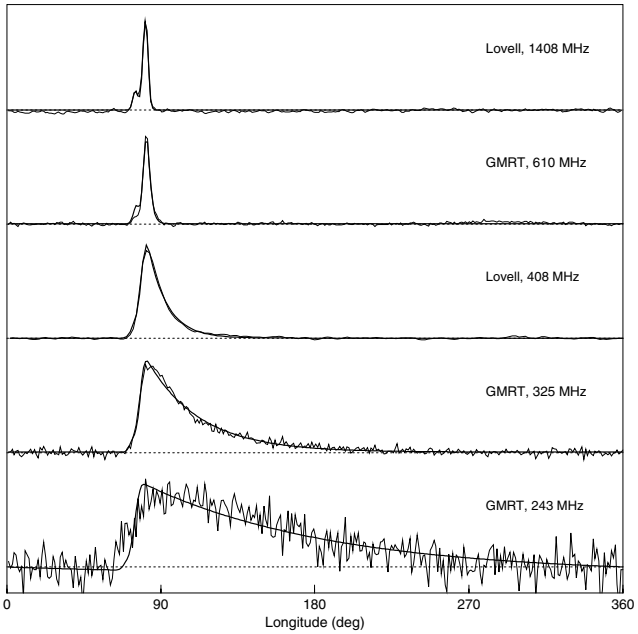

Fig. 1. Integrated pulse profiles and best-fit model profiles for PSR B1831−03 at different frequencies. The profiles at 243, 325 and 610 MHz were observed with the GMRT, whereas the 408 and 1408 MHz profiles were taken from the EPN database (Lovell observations). The alignment of the profiles for different frequencies was done with respect to the peak of the main pulse.

best fit of the model profile, which is the convolution of the template with the dispersion smearing and the adopted PBFs, to the observed profile. The exact functional form for the PBF of the ISM is not known. We thus analyse the fits for three trial PBFs; (1) the PBF for a thin screen (PBF_1); and (2) for a uniformly distributed medium (PBF_2) in an ISM with Gaussian density fluctuations, given by (Williamson 1972, 1973):

$$PBF_1(t) = \exp(-t/\tau_d)\, U(t) \quad (3)$$

$$PBF_2(t) = (\pi^5 \tau_d^3/8t^5)^{1/2} \exp(-\pi^2 \tau_d/4t)\, U(t), \quad (4)$$

where $U(t)$ is the unit step function, i.e. $U(t < 0) = 0, U(t \geq 0) = 1$. (3) The third PBF is characterized by density fluctuations with a Lévy probability distribution function that has a power-law decay (Boldyrev & Gwinn 2003) and an asymptotic form $PBF_3(t) = (t/\tau_d)^{-4/3}\, U(t)$ for $t/\tau_d \gg 1$. As for the high DM pulsars presented in Paper I, we again find PBF_1 to be most appropriate to describe the observed scattering. In particular, the fits using PBF_2 and PBF_3 cannot reproduce the long "scattering tails" observed at lower frequencies, resulting in χ^2 values that are larger by factors of 2 and more. Using the thin screen approximation we obtain best-fit values and uncertainties for τ_d from the χ^2 contours in the plane of τ_d and offset in phase.

In Fig. 1 observed and best-fit model profiles for the observed frequencies are shown for PSR B1831−03. The template is constructed from the 1408 MHz Lovell profile using two Gaussians. Note the high S/N ratio and quality of the GMRT profiles proving that this new telescope is highly capable of pulsar observations at low radio frequencies. The best-fit model profiles describe the shape of the observed profiles in an excellent manner. At 610 MHz the small peak at the leading part of the profile was not observed, which, however, does not affect the τ_d measurement (see next paragraph). At 243 MHz the dispersion smearing at the leading part of the profile seems to be not adequately described by the model profile, resulting in a much steeper rise of the peak. We repeated the fit using artificially increased dispersion smearing functions and found that the effect on τ_d is well below its 1σ uncertainty and therefore negligible.

As noted in Paper I, intrinsic profile variations with frequency (see the 610 MHz profile of Fig. 1) could in principle give rise to inaccurate estimation of pulse broadening times. A careful analysis of these effects on the measured τ_d can be done using simulated pulse profiles with frequency evolution that are made subject to pulse broadening. As shown, resulting deviations of the measured τ_d values from the true ones are in fact very small and can be accounted for using increased error bars. Thus, we again quote conservative 3σ error bars for all scatter broadening times.

Recently, another method to analyse pulse broadening related to the CLEAN alogrithm was proposed by Bhat et al. (2003). In their approach, the authors try to derive the intrinsic pulse shape at the observed frequency without using any knowledge of the pulse profile at another, higher frequency. They point out that utilizing a high frequency template can indeed lead to uncertainties due to the same unkown frequency evolution of the pulse profile that we try to simulate in our computations (see Paper I). Whilst it is indeed more straightforward in their method to perform a deconvolution to recover the intrinsic profile, their alogrithm cannot always produce unique results, yielding strikingly different values and hence uncertainties, sometimes. This is demonstrated for PSR B1849+00 which was also studied in Paper I. Applying PBF_1 and PBF_2 (see Eqs. (3) and (4)) the authors obtain equally good fits for $\tau_d = 225 \pm 14$ ms and $\tau_d = 121 \pm 6$ ms, where a choice can only be made by making an assumption about the more likely intrinsic profile. A comparison of these values with our measurement of $\tau_d = 223 \pm 24$ ms as derived in Paper I shows that both methods result in consistent pulse broadening times for the case of the thin screen approximation. This supports our findings that an exponential decay is the most appropriate form to describe pulse broadening for intermediate and high DM pulsars. The example of PSR B1849+00 shows that extra, a priori information (typically an idea of the expected pulse shape) is usually needed to obtain correct solutions for more complicated profiles which holds true for both the CLEAN algorithm as well as our approach. Given the apparent imperfections of both methods, all derived values should be treated with considerable care, e.g. by reflecting the possible systematic errors by increasing the error estimates correspondingly, as done in our study. It is comforting to note that for PSR B1849+00 the frequency dependence of τ_d, derived by Bhat et al. (2003, $\alpha = 3.5 \pm 0.7$), and us (Paper I, $\alpha = 2.8^{+1.0}_{-0.6}$) are consistent. Recent OH observations toward PSR B1849+00 revealed absorption features that most likely originate from a small and dense molecular clump (Stanimirović et al. 2003). Thus, the LOS to the pulsar probes complex material so that our findings of non-Kolmogorov frequency dependence of pulse broadening is not surprising.

Table 1. Pulse broadening measurements.

PSR	l	b	DM	D	τ_{243}	τ_{325}	τ_{408}	τ_{610}	α	β	$\log C_{n_e}^2$
	(deg)	(deg)	(pc cm^{-3})	(kpc)	(ms)	(ms)	(ms)	(ms)			
(1)	(2)	(3)	(4)	(5)	(6)	(7)	(8)	(9)	(10)	(11)	(12)
B1821−19	12.3	−3.1	224	4.7	...	58 (23)	22 (4)	4.6 (0.2)	$4.0^{+0.5}_{-0.7}$	$4.0^{+1.1}_{-0.4}$	−1.1
B1826−17	14.6	−3.4	218	4.7	...	137 (37)	41 (6)	7.5 (1.3)	$4.6^{+0.5}_{-0.5}$	$3.6^{+0.4}_{-0.2}$	−0.9
B1831−03	27.7	2.3	236	5.2	208 (94)	59 (4)	21.3 (1.1)	3.2 (0.5)	$4.5^{+0.4}_{-0.6}$	$3.6^{+0.5}_{-0.2}$	−1.2
B1845−01	31.3	0.0	159	4.0	...	262 (181)	54 (8)	17.0 (1.4)	$4.3^{+0.7}_{-1.2}$	$3.8^{+1.9}_{-0.4}$	−0.5
B1859+03	37.2	−0.6	401	7.3	...	241 (51)	89 (9)	12.6 (0.9)	$4.7^{+0.3}_{-0.4}$	$3.5^{+0.2}_{-0.1}$	−1.0
B1900+01	35.7	−2.0	246	3.4	176 (58)	34 (2)	14.7 (1.3)	<1.0	$4.8^{+0.6}_{-0.8}$	$3.4^{+0.6}_{-0.2}$	−1.0
B1920+21	55.3	2.9	217	7.6	4.5 (1.5)	<0.8	<1.7	<0.6	...	...	−2.9
B1933+16	52.4	−2.1	159	5.6	4.6 (0.2)	1.8 (0.1)	<1.9	<0.4	$3.4^{+0.2}_{-0.2}$	...	−2.7
B2002+31	69.0	0.0	235	7.5	27 (13)	5.3 (1.2)	2.0 (1.4)	<0.7	$5.0^{+1.7}_{-1.5}$	$3.3^{+1.3}_{-0.5}$	−2.3

Note: Columns 2 and 3 give the Galactic longitude and latitude of each pulsar; Col. 4 its Dispersion Measure (DM) and Col. 5 its DM distance (from the Cordes & Lazio 2002 model, hereafter NE2001); Cols. 6–9 the pulse broadening times with 3σ errors in parenthesis at 243, 325, 408 and 610 MHz. Upper limits are quoted with "<". Column 10 gives the spectral index of pulse broadening and Col. 11 the spectral index of density irregularities (using $\beta = 2\alpha/(\alpha - 2)$) for each pulsar with their 1σ errors. Column 12 gives the logarithm of the fluctuation strength $C_{n_e}^2$.

3. Results and discussion

Table 1 summarises the multi-frequency measurements of pulse broadening times for our sample of pulsars. PSRs B1821-19 and B1859+03 were not observed at 243 MHz due to the limited telescope time. For PSRs B1826−17 and B1845−01 we did not detect a pulse profile at this frequency, probably because the pulse is smeared due to high scattering.

Figure 2 shows the measured frequency dependence of τ_d. For all pulsars with more than one τ_d measurement, i.e. for all but PSR B1920+21, we calculated the spectral index of pulse broadening, α, from Monte-Carlo simulations as described in Paper I. For PSR B1933+16, we used values of $\tau_d = 67(13)$ ms at 110 MHz and $\tau_d = 25(4)$ ms at 160 MHz from the literature (Rickett 1977; Slee et al. 1980). The median α and its 1σ errors are listed in Table 1. Also listed are the spectral indices of the electron density spectrum, β, which we calculated from the relation $\beta = 2\alpha/(\alpha - 2)$. Note that this relation is only valid for $\beta < 4$, i.e. for all our pulsars except PSR B1933+16. The average spectral index for seven pulsars (excluding PSRs B1920+21 and B1933+16) is $\langle\alpha\rangle = 4.57 \pm 0.09$. Figure 3 shows the spectral index of pulse broadening as a function of DM for our measurements as well as published data. All of our new spectral indices, except the one for PSR B1933+16, are consistent within their errors with the Kolmogorov value of 4.4, as found for most of the low DM pulsars as well. However, along several LOSs, as towards the Crab and Vela pulsar, PSR B1933+16 and the high DM pulsars, the Kolmogorov theory fails leading to flattening of the spectra of scatter broadening. The results for the Crab and Vela pulsar are not surprising, as the complex structure of the surrounding supernova remnants can introduce a number of effects affecting the observed scattering properties (e.g. Backer et al. 2000; Lyne et al. 2001).

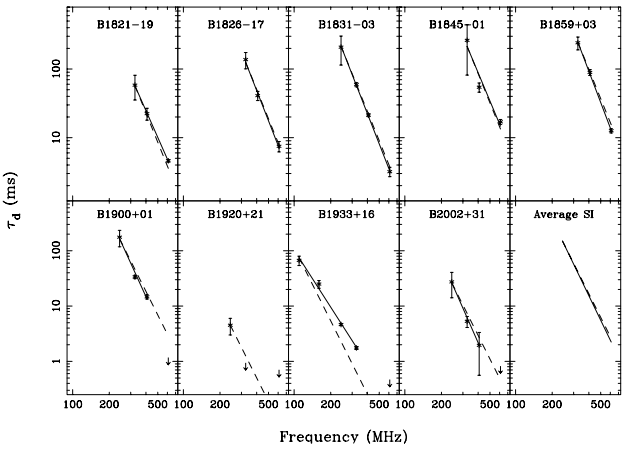

Fig. 2. Pulse broadening times, τ_d, with their 3σ errors as a function of observing frequency, ν, for nine pulsars. Arrows denote measured upper limits on τ_d. The lines correspond to the linear fit of the form $y = -\alpha\, x + K$ where $y = \log(\tau_d)$ in ms and $x = \log(\nu)$ in MHz. The dashed lines are examples of the expected dependence due to a Kolmogorov spectrum, i.e. $\alpha = 4.4$. The bottom right most panel shows a linear function with the derived average spectral index $\langle\alpha\rangle = 4.57$. See text for further details.

The spectral index of pulse broadening for the LOS to PSR B1933+16 is $\alpha = 3.4(2)$, i.e. significantly lower than the Kolmogorov value of 4.4. This measured flattening of the spectrum has been observed before for high DM pulsars and can be explained by anomalous scattering at multiple scattering screens with finite extensions and/or varying scattering strength (see Paper I). Our pulse broadening measurements for PSR B1933+16 along with published τ_d's at 110 and 160 MHz fit excellently to a power-law model with $\log(\tau_d(\mathrm{ms})) = -3.4\,\log(\nu) + 8.9$, where ν is in MHz (as

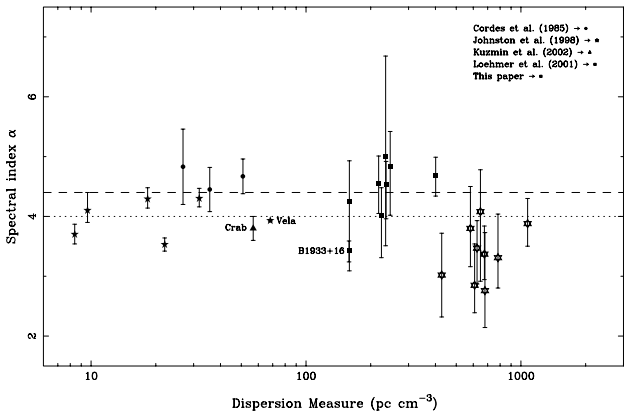

Fig. 3. Spectral index of pulse broadening, α, as a function of dispersion measure, DM, for the current sample as well as for earlier measurements (Cordes et al. 1985; Johnston et al. 1998; Löhmer et al. 2001; Kuzmin et al. 2002). The dashed line $\alpha = 4.4$ indicates the spectral index for a Kolmogorov spectrum. The dotted line $\alpha = 4.0$ represents the spectral index for a Gaussian distribution of irregularities.

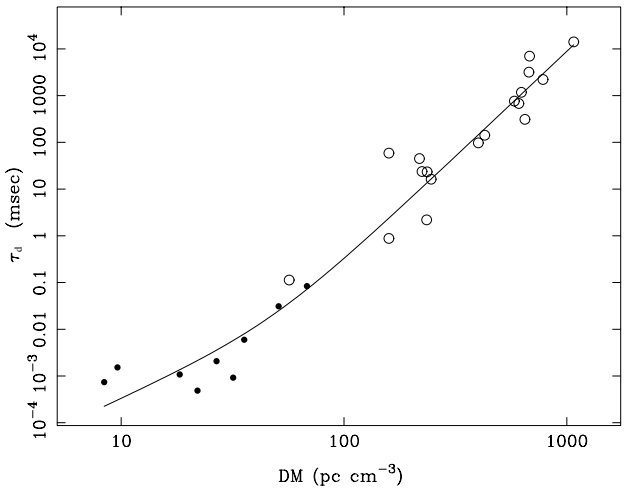

Fig. 4. Pulse broadening times, τ_d, versus dispersion measure, DM, for 27 pulsars as plotted in Fig. 3. Filled circles corresponds to decorrelation bandwidth measurements and open circles are pulse broadening measurements. The solid line corresponds to the best fit given by Eq. (5). See text for further details.

seen in Fig. 2). It should be noted that combining measurements at different epochs can be affected by refractive scintillations which may alter τ_d between epochs and thereby alter values of α. However, our τ_d measurements being quasi simultaneous (separated by days) are unlikely to be affected by refractive scintillations and the spectrum derived by these values is in good agreement with the low frequency values obtained by Cordes et al. (1985) at an earlier epoch. The authors quote $\Delta\nu_d$ values for this pulsar near closeby frequencies of 1.41, 1.42, and 1.67 GHz as 0.125, 0.100, and 0.110 MHz, respectively. We extrapolated our τ_d spectrum to these frequencies, solved Eq. (1) for C_1 and found it to be 9.1, 7.1, and 4.5, respectively, i.e. much larger than unity. The $\Delta\nu_d$ measurements could have been biased by refractive ISS (e.g. Gupta et al. 1994) leading to an underestimation of the true bandwidths. The resulting smaller values of τ_d at these frequencies, however, would lead to a steeper spectrum or to higher C_1 values making the discrepancy even worse[3]. Our measured C_1's are much greater than unity and therefore in contradiction to what is predicted by standard theories of the ISM. Lambert & Rickett (1999), for instance, tabulated possible values for different geometries and spectral models and found values ranging from 0.56 to 1.53, i.e. still much smaller than those for PSR B1933+16. However, if we were to apply a Kolmogorov spectrum ($\alpha = 4.4$) – even though it is a very poor fit to the data – the extrapolated τ_d's for PSR B1933+16 would be much smaller at the corresponding frequencies, resulting in C_1's that are much smaller, eventually even smaller than unity. Thus, the LOS to PSR B1933+16 remains to be an unresolved puzzle. Careful observations of decorrelation bandwidths of this pulsar in the frequency range of 300−1400 MHz are needed to help understanding the properties of the ISM along this LOS.

[3] Note that there is a possibility that the nature of the PBF may evolve from the well established exponential form, in the regime where $\Delta\nu_d$ is the easier quantity to measure. However, there is no evidence of this from the main theoretical models (e.g. Lambert & Rickett 1999, and references therein).

One of the conventional methods of examining the scattering properties along various LOSs is to investigate the relation between the measured pulse broadening and the DM. Considering DM as proportional to the distance D to the pulsar, the power law model of density irregularities predicts $\tau_d \propto (C_{n_e}^2)^{2/(\beta-2)}\,\mathrm{DM}^{\beta/(\beta-2)}\,\nu^{-2\beta/(\beta-2)}$, which reduces to $\tau_d \propto (C_{n_e}^2)^{1.2}\,\mathrm{DM}^{2.2}\,\nu^{-4.4}$ for the Kolmogorov spectrum with $\beta = 11/3$ (Romani et al. 1986). Sutton (1971) first noted that, for DM $\lesssim$ 20, τ_d increases roughly as DM^2, but for 20 $\lesssim$ DM $\lesssim$ 400 the relation steepens approaching DM^4. With many more available measurements of τ_d (and $\Delta\nu_d$) this relation has been revisited (e.g. Rickett 1977; Ramachandran et al. 1997). However, the basic feature of flatter and steeper slopes for low and high DM pulsars seems to hold well. In most of these studies the measured τ_d or $\Delta\nu_d$ are scaled to a reference frequency assuming a a priori frequency dependence of $\nu^{4.4}$. In Fig. 4 we show a plot of τ_d versus DM at 400 MHz for all the pulsars where the frequency scaling is now measured, i.e. all pulsars from Fig. 3. We have fitted the empirical function $\tau_d\,(\mathrm{ms}) = A\,\mathrm{DM}^{\gamma}\,(1 + B\,\mathrm{DM}^{\zeta})$, as was suggested by Ramachandran et al. (1997). Here the term $(1 + B\,\mathrm{DM}^{\zeta})$ should provide a useful description for the apparent mean dependence of the level of turbulence on DM. In order to assess the deviation from the Kolmogorov value we fixed $\gamma = 2.2$, and derived a best fit of the form

$$\tau_d\,(\mathrm{ms}) = 2.5 \times 10^{-6}\,\mathrm{DM}^{2.2}\,(1 + 1.34 \times 10^{-4}\,\mathrm{DM}^{2.3}) \qquad (5)$$

which is shown by solid line in Fig. 4. Comparing our results with the fit obtained by Ramachandran et al. (1997), their best-fit curve is slightly shifted to higher τ_d values, most probably caused by the large scatter of data points. The exponent ζ is somewhat smaller than their value of 2.5, leading to a flattening of the curve at the highest DMs. As the high DM pulsars have frequency scaling laws which are significantly smaller than 4.4 (see Paper I), the extrapolation of their spectrum down to 400 MHz leads to lower τ_d values than

for the case of a Kolmogorov spectrum. This explains the flattening of the τ_d–DM curve at the high DM end. However, the large scatter in the τ_d values and small number statistics do not allow a tighter constraint of ζ. The different slopes for low and high DM pulsars have been studied in detail by several investigators (e.g. Rickett 1977; Cordes et al. 1985; Rickett 1990). An extra bias could be introduced by a wrong conversion of $\Delta\nu_d$ to τ_d for the low DM pulsars. Indeed, if $C_1 \sim 1$ (see Eq. (1)) does not hold, a comparison of the $\Delta\nu_d$ and τ_d measurements is not possible. However, if C_1 differs from unity by a constant amount, all points are shifted in the τ_d versus DM plot to one direction by a fixed factor. Only a systematic change in C_1 with DM could change the slope of the curve itself. However, as was discussed by Rickett (1977), theoretically there is very little flexibility in changing C_1 from values close to unity. The only experimental confirmation for this became available for the Vela pulsar by Backer (1974), who found $C_1 = 1.07$ by extrapolating several τ_d and $\Delta\nu_d$ measurements at a given frequency. For PSR B1933+16, however, as discussed earlier, it appears that there is some evidence for C_1 values greater than unity.

Alternatively, if we accept $C_1 \sim 1$, one can in principle explain the steeping in the τ_d versus DM relation by proposing a breakdown of the homogeneity condition in the medium (Rickett 1977). A usual way to check this condition is to analyse the scattering strength $C^2_{n_e}$ along the LOS. For a homogeneous medium with a Kolmogorov spectrum, $C^2_{n_e}$ can be found by using the definition from Cordes (1986), as

$$C^2_{n_e}(\mathrm{m}^{-20/3}) = 0.002\,\nu^{11/3}\,D^{-11/6}\,\Delta\nu_d^{-5/6}, \quad (6)$$

with ν in GHz, D in kpc and $\Delta\nu_d$ in MHz. We used Eq. (6) to calculate $C^2_{n_e}$ for the pulsars from this paper and Paper I, by averaging over all frequencies. Our τ_d values were converted to $\Delta\nu_d$ using $C_1 = 1.16$, the value appropriate for a uniform medium and having a Kolmogorov spectrum (Cordes & Lazio 2002). The distances were obtained from the Cordes & Lazio (2002) model of the Galactic electron density distribution, hereafter NE2001. $C^2_{n_e}$ for other pulsars were used from Johnston et al. (1998) and Cordes et al. (1985), but scaled appropriately for the new NE2001 model distances. In Fig. 5 we plot the scattering strength $C^2_{n_e}$ as a function of distance for all the 27 pulsars with known frequency scaling law. As clearly seen in the top panel, $C^2_{n_e}$ increases with distance, a result which is consistent with that of Cordes et al. (1985). For a homogeneous medium one expects to find $\log(C^2_{n_e})$ near its canonical value of −3.5 (e.g. Johnston et al. 1998), which is only true for the nearby pulsars. Instead, for most of the sources with $D \gtrsim 3$ kpc, we find values much larger than −3.5 indicating that we sample highly dense regions with enhanced scattering along these LOSs. As seen in the bottom panel of Fig. 5, the LOSs with enhanced scattering strength are concentrated in the inner regions of the Galaxy where the majority of HII regions can be found. These LOSs additionally show flatter spectra of pulse broadening indicating multiple scattering screens of anisotropic irregularities (Paper I).

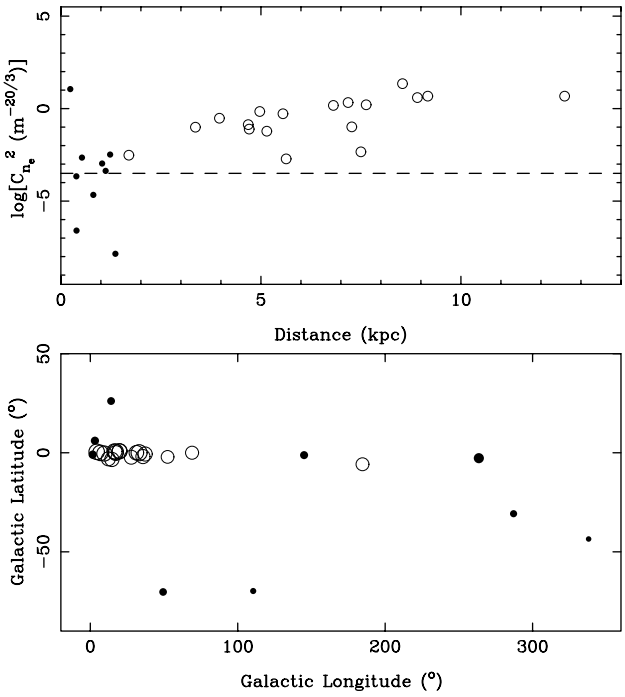

Fig. 5. The top panel shows scattering strength $\log(C^2_{n_e})$ versus distance for 27 pulsars as in Fig. 3. The dashed line corresponds to −3.5, the canonical value for a homogeneous Kolmogorov medium. The bottom panel shows the LOSs for these pulsars in the Galaxy, where the size of the circles corresponds to the magnitude of $C^2_{n_e}$. The filled circles indicate decorrelation bandwidth measurements and the open circles are pulse broadening measurements. See text for further details.

4. Summary and conclusions

We have presented measurements of pulse broadening times for a sample of intermediate DM pulsars. The obtained results bridge the gap in the available literature from low DM to high DM pulsars. For both the high DM pulsars presented in Paper I and the current sample, we find that the PBF for a Gaussian distribution of irregularities and applying the thin screen approximation is most appropriate to describe the observed scattering. While there are significant deviations from the expected frequency scaling for high DM pulsars (Paper I), our current sample is, apart from the exception for PSR B1933+16, consistent with a Kolmogorov spectrum. Therefore, we conclude that LOSs to pulsars with $0 \lesssim \mathrm{DM} \lesssim 300$ pc cm^{-3} show pulse broadening that is consistent with a Kolmogorov spectrum of electron density irregularities (except for a few pulsars with complicated LOSs, e.g. the Crab and Vela pulsars, PSR B1933+16). At around DM = 300 pc cm^{-3} a change in the spectral index of pulse broadening is observed leading to a flattening of the spectra. We think that this change is related to a change of the Galactic material in the inner region of the Galaxy. Future multi-frequency observations are highly desirable to probe the DM range of 250–400 pc cm^{-3} and to determine the exact transition point.

Standard theory appears still to be challenged by our result for the relationship connecting the pulse broadening time with the decorrelation bandwidth. Mostly only one of these quantities is measurable, while the other is computed using an

assumed standard relation. This can obviously lead to systematic errors which need to be considered when combining corresponding data sets. Nevertheless, such procedure may be still unavoidable in order to increase the size of the studied sample, since the results obtained here and in Paper I underline the impression that the overall state of the ISM can only be determined in a statistical sense. Clearly, individual results are affected by the properties of certain LOSs. For this reason, special care is needed when interpreting the results obtained only for a small sample of pulsars.

Acknowledgements. We thank the staff of the GMRT for help with the observations. The GMRT is run by the National Centre for Radio Astrophysics of the Tata Institute of Fundamental Research. We would also like to thank the referee for useful suggestions that helped to improve the text.

References

Armstrong, J. W., Rickett, B. J., & Spangler, S. R. 1995, ApJ, 443, 209
Backer, D. C. 1974, ApJ, 190, 667
Backer, D. C., Wong, T., & Valanju, J. 2000, ApJ, 543, 740
Bhat, N. D. R., Cordes, J. M., & Chatterjee, S. 2003, ApJ, 584, 782
Bhat, N. D. R., Gupta, Y., & Rao, A. P. 1999, ApJ, 514, 249
Boldyrev, S., & Gwinn, C. 2003, ApJ, 584, 791
Cordes, J. M. 1986, ApJ, 311, 183
Cordes, J. M., & Lazio, T. J. W. 2001, ApJ, 549, 997
Cordes, J. M., & Lazio, T. J. W. 2002, ApJ, submitted [arXiv:astro-ph/0207156]
Cordes, J. M., Weisberg, J. M., & Boriakoff, V. 1985, ApJ, 288, 221
Gould, D. M., & Lyne, A. G. 1998, MNRAS, 301, 235
Gupta, Y. 2000, in Pulsar Astronomy – 2000 and Beyond, IAU Coll. 177, ed. M. Kramer, N. Wex, & R. Wielebinski (San Francisco: ASP), 539
Gupta, Y., Gothoskar, P., Joshi, B. C., et al. 2000, in Pulsar Astronomy – 2000 and Beyond, IAU Coll. 177, ed. M. Kramer, N. Wex, & R. Wielebinski (San Francisco: ASP), 277
Gupta, Y., Rickett, B. J., & Lyne, A. G. 1994, MNRAS, 269, 1035
Johnston, S., Nicastro, L., & Koribalski, B. 1998, MNRAS, 297, 108
Kuzmin, A. D., Kondrat'ev, V. I., Kostyuk, S. V., et al. 2002, Astron. Lett., 28, 251
Lambert, H. C., & Rickett, B. J. 1999, ApJ, 517, 299
Löhmer, O., Kramer, M., Mitra, D., Lorimer, D. R., & Lyne, A. G. 2001, ApJ, 562, L157 (Paper I)
Lyne, A. G., Pritchard, R. S., & Graham-Smith, F. 2001, MNRAS, 321, 67
Ramachandran, R., Mitra, D., Deshpande, A. A., McConnell, D. M., & Ables, J. G. 1997, MNRAS, 290, 260
Rickett, B. J. 1977, Ann. Rev. Astr. Ap., 15, 479
Rickett, B. J. 1990, Ann. Rev. Astr. Ap., 28, 561
Romani, R. W., Narayan, R., & Blandford, R. 1986, MNRAS, 220, 19
Scheuer, P. A. G. 1968, Nature, 218, 920
Slee, O. B., Dulk, G. A., & Otrupek, R. E. 1980, PASA, 4, 100
Stanimirović, S., Weisberg, J. M., Dickey, J. M., et al. 2003, ApJ, 592, 953
Sutton, J. M. 1971, MNRAS, 155, 51
Swarup, G., Ananthakrishnan, S., Subrahmanya, C. R., et al. 1997, in High-Sensitivity Radio Astronomy, ed. N. Jackson, & R. J. Davis (Cambridge University Press)
Taylor, J. H., & Cordes, J. M. 1993, ApJ, 411, 674
Taylor, J. H., Manchester, R. N., & Lyne, A. G. 1993, ApJS, 88, 529
Thorsett, S. E. 1991, ApJ, 377, 263
Williamson, I. P. 1972, MNRAS, 157, 55
Williamson, I. P. 1973, MNRAS, 163, 345